EUROPEAN ORGANIZATION FOR NUCLEAR RESEARCH

L3 Note 2573
July 10, 2000

Search for Neutral Higgs Bosons of the Minimal Supersymmetric Standard Model in e^+e^- Interactions at $\sqrt{s} = 192$ - 202 GeV

The L3 Collaboration

Abstract

A search for the lightest neutral CP-even and neutral CP-odd Higgs bosons in the Minimal Supersymmetric Standard Model is performed using 233.2 pb^{-1} of integrated luminosity collected by L3 at center-of-mass energies 192 - 202 GeV. No signal is observed. Lower limits on the masses of neutral Higgs bosons are given as a function of tanβ within the maximal mixing and no mixing scenarios. For tanβ greater than 0.8, the lower mass limits at 95% confidence level are $m_{\mathrm{h}} > 82.6$ GeV and $m_{\mathrm{A}} > 83.0$ GeV. For $0.8 < \tan\beta < 1.6$, values of m_{A} up to 1 TeV are excluded in both mixing scenarios thus ruling out this region of tanβ in the MSSM.

Submitted to the *XXXth International Conference on High Energy Physics*
July 27 - August 2, 2000, Osaka, Japan

Introduction

In the Minimal Supersymmetric Standard Model (MSSM) [1] two Higgs doublets are required, giving rise to five Higgs bosons: a charged scalar pair; two neutral CP-even, the lightest of which is called h; and a neutral CP-odd, A. We consider here the two production mechanisms which are the most important at LEP :

$$\mathrm{e^+e^- \rightarrow Z^* \rightarrow hZ} \tag{1}$$
$$\mathrm{e^+e^- \rightarrow Z^* \rightarrow hA.} \tag{2}$$

The cross section of (1) is, in general, smaller than that for the production of the Higgs boson in the Standard Model, but in the MSSM pair-production of Higgs bosons (2) appears.

Previous searches for the h and A bosons have been reported by L3 [2] and other experiments [3]. This paper presents analyses done on the data collected by L3 in 1999 at $\sqrt{s} = 192 - 202$ GeV. The sensitivity of MSSM neutral Higgs boson searches is improved by combining the results of these analyses with previous searches.

Data and Monte Carlo Samples

In 1999 the data were taken by the L3 detector [4] at center-of-mass energies ranging from 192 to 202 GeV. The luminosities collected at each center-of-mass energy are reported in table 1.

The cross sections of processes (1) and (2) and decay branching ratios of h and A are calculated using the HZHAv3.0 generator [5]. For the efficiency studies, Monte Carlo samples of Higgs events are generated using PYTHIA [6] and HZHA. For the background studies, the following Monte Carlo programs are used: PYTHIA ($\mathrm{e^+e^- \rightarrow q\bar{q}(\gamma)}$), KORALW [7] ($\mathrm{e^+e^- \rightarrow W^+W^-}$), KORALZ [8] ($\mathrm{e^+e^- \rightarrow \tau^+\tau^-}$), PYTHIA and PHOJET [9] ($\mathrm{e^+e^- \rightarrow e^+e^- q\bar{q}}$), EXCALIBUR [10] ($\mathrm{e^+e^- \rightarrow f\bar{f}'f''\bar{f}'''}$) and PYTHIA ($\mathrm{e^+e^- \rightarrow ZZ}$ and $\mathrm{e^+e^- \rightarrow Ze^+e^-}$).

The L3 detector response is simulated using the GEANT 3.15 program [11], which takes into account the effects of energy loss, multiple scattering and showering in the detector. The GHEISHA program [12] is used to simulate hadronic interactions in the detector.

center-of-mass energy	$\int$ Ldt , $\mathrm{pb^-1}$
192	29.7
196	83.7
200	82.8
202	37.0

Table 1: The integrated luminosities collected by L3 at different center-of-mass energies.

Analysis Procedures

The search for hA and hZ production is carried out within the constrained MSSM assuming unification of the scalar fermion masses, the gaugino masses and the trilinear Higgs-fermion couplings at the GUT scale. This choice has little impact on the phenomenology of Higgs bosons but reduces significantly the number of free parameters. The free parameters are chosen to be the ratio of two Higgs vacuum expectation values, tanβ; the mass of CP-odd Higgs boson, m_{A}; the gaugino mass parameter, M_2; the universal scalar fermion mass, m_0; the common squark trilinear coupling, A; and the Higgs mixing parameter, μ.

Two benchmark scenarios [13] are considered. In the first scenario, called "maximal mixing scenario", the mixing in the scalar top sector is large and the MSSM parameters are chosen such that the mass of the lightest neutral CP-even Higgs boson, m_{h}, acquires the maximal value as function of tanβ. The second scenario corresponds to vanishing mixing in the scalar top sector and is usually refered to as "no mixing scenario".

We used for the calculation of radiative corrections at two-loop level the HZHA v3.0 generator, which is based on the renormalisation group method. The MSSM parameters are chosen as follows: $m_0 = 1$ TeV, $\mu = -200$ GeV, $M_2 = 200$ GeV. The mass of top quark m_{top} is fixed to 175 GeV. Within the framework of the renormalisation group approach the maximal mixing scenario is realized at $X_t = A - \mu \cot\beta = \sqrt{6}$ TeV, where X_t is the parameter which controls the mixing in the stop sector. No mixing scenario coresponds to $X_t = 0$. Finally, a scan over the two remaining independent parameters, tanβ and m_{A}, is performed in each mixing scheme in the ranges: $0.5 \leq \tan\beta \leq 50$; 10 GeV $\leq m_{\mathrm{A}} \leq$ 1 TeV.

The two Higgs production mechanisms, $\mathrm{e^+e^-} \to \mathrm{Z}^* \to \mathrm{hA}$ and $\mathrm{e^+e^-} \to \mathrm{Z}^* \to \mathrm{hZ}$, vary in relative importance as a function of tanβ. The production of hA is dominant at high tanβ, while hZ production is dominant at low tanβ.

In the case of hZ, four event topologies representing, approximately 98% of possible final states, are considered : $\mathrm{q\bar{q}q\bar{q}}$, $\mathrm{q\bar{q}}\nu\bar{\nu}$, $\mathrm{q\bar{q}l^+l^-}(\mathrm{l} = \mathrm{e}, \mu, \tau)$ and $\tau^+\tau^-\mathrm{q\bar{q}}$. The analyses including hadronic h decays were optimized for the $\mathrm{h} \to \mathrm{b\bar{b}}$ decay channel but the efficiencies of decay modes $\mathrm{h} \to \mathrm{c\bar{c}}, \mathrm{gg}$ are also considered. The analyses $\mathrm{q\bar{q}}\nu\bar{\nu}$ and $\mathrm{q\bar{q}l^+l^-}(\mathrm{l} = \mathrm{e}, \mu)$ are the same as in SM Higgs searches [14]. The analyses $\mathrm{hZ} \to \mathrm{q\bar{q}q\bar{q}}$ and $\mathrm{hZ} \to \mathrm{q\bar{q}}\tau^+\tau^-(\tau^+\tau^-\mathrm{q\bar{q}})$ do not overlap with similar modes in the hA channel : $\mathrm{hA} \to \mathrm{b\bar{b}b\bar{b}}$ and $\mathrm{hA} \to \mathrm{b\bar{b}}\tau^+\tau^-(\tau^+\tau^-\mathrm{b\bar{b}})$.

Common search procedures are applied to both the hA and hZ search channels. First, a preselection is applied which significantly reduces background while keeping the signal efficiency high. This is especially effective against background from the two photon interaction, which has a large cross section at these LEP energies. Second, a final selection is chosen to distinguish signal from background. Once the final selection has been applied, a discriminating variable based on likelihood is defined as in Reference [15]. For the channels $\mathrm{hA} \to \mathrm{b\bar{b}b\bar{b}}$ and $\mathrm{hZ} \to \mathrm{b\bar{b}q\bar{q}}$ an analysis based on neural network techniques is also used and decribed below. The two analyses give similar results.

The $\mathrm{hA} \to \mathrm{b\bar{b}b\bar{b}}$ and $\mathrm{hZ} \to \mathrm{b\bar{b}q\bar{q}}$ channels

The signature of both the $\mathrm{hA} \to \mathrm{b\bar{b}b\bar{b}}$ and $\mathrm{hZ} \to \mathrm{b\bar{b}q\bar{q}}$ final states is four hadronic jets and the presence of b-hadrons. The dominant backgrounds come from $\mathrm{q\bar{q}}(\gamma)$ production and hadronic decays of W and Z pairs. In the case of $\mathrm{hA} \to \mathrm{b\bar{b}b\bar{b}}$, the identification of b-hadrons plays an especially important role.

First, a high multiplicity hadronic preselection, common to both hA and hZ, is applied at each center-of-mass energy. At least 20 tracks and 35 calorimetric clusters are required; the visible energy must be greater than $0.6\sqrt{s}$ and less that $1.4\sqrt{s}$; events with perpendicular imbalances greater than $0.35\mathrm{E_{vis}}$ are rejected, where $\mathrm{E_{vis}}$ is the visible energy. A cut is applied on the maximal lepton energy, $E^{\mathrm{l}}_{\mathrm{max}} < 65$ GeV to suppress semileptonic W pair decays. Hadronic events with initial state radiation are further suppressed by requiring $P^{\mathrm{L}}_{\mathrm{mis}}/(m_{\mathrm{vis}} - m_{\mathrm{Z}}) < 0.4$, where $P^{\mathrm{L}}_{\mathrm{mis}}$ is the longitudinal component of missing momentum, m_{vis} is the visible mass and m_{Z} the Z boson mass. Events passing the preselection are then forced to four jets using the DURHAM [16] clustering algorithm and a kinematic fit requiring 4-momentum conservation (4C) is performed. The number of expected and observed events in the $\sqrt{s} = 192 - 202$ GeV data along with the signal efficiencies for the preselection cuts are listed in Table 2.

After preselection the most discriminating event variables are combined into a feed forward neural network [17], with one hidden layer and three output nodes. The inputs include the probability that the jets contain b-quarks [18], hereafter called $\mathrm{B_{Tag}}$, event shape variables and mass information. The information on event shape include the event spherocity, the value of the DURHAM jet resolution parameter for which the event goes from the four-jet to three-jet topology, the longitudinal component of missing momentum and the event thrust. The mass information is used as input to the network by means of the χ^2 variable defined as follows:

$$\chi^2(m_X, m_h) = \Big((\Sigma_{ij}^{min} - (m_X + m_h))^2 w_\Sigma + (\Delta_{ij}^{min} - |m_X - m_h|)^2 w_\Delta)\Big) \qquad (3)$$

where $\mathrm{m_X}$ is either $\mathrm{m_Z}$ or $\mathrm{m_A}$, Σ_{ij} is the sum of the dijet masses and Δ_{ij} the difference between the dijet masses. The pairing is used, which gives the minimum value for the difference squared $(\Delta_{ij} - |m_X - m_h|)^2$ between the measured and expected dijet mass differences, and $\Sigma^{\mathrm{min}}_{\mathrm{ij}}$ is the corresponding sum of the dijet masses. The weights, w_Σ and w_Δ, reflect the typical mass resolutions. In this way, the shape of the neural network output is made almost independent of the mass hypotesis. In case of the hA analysis the polar angle of the Higgs boson, Θ, is also used as input. This gives additional separation between hA signal and WW background due to the spin difference between W and Higgs bosons. The three output variables of the neural network correspond to the signal, $\mathrm{O_{higgs}}$, the $\mathrm{q\bar{q}}(\gamma)$ final state, $\mathrm{O_{qq}}$, and the WW final states, $\mathrm{O_{WW}}$. The final discriminating variable is then obtained from the combination $\mathrm{NN} = \mathrm{O_{higgs}} \cdot (1 - \mathrm{O_{qq}}) \cdot (1 - \mathrm{O_{WW}})$. Two independent neural networks are used for the hZ and hA analyses, and events are then classified in one of the two categories according to the final variable with larger value.

The distribution of the most discriminating input variables, namely the $\mathrm{B_{Tag}}$ variable, the mass χ^2 and the reconstructed polar angle of the boson, are shown in Figure 1. The final variable distribution is shown in Figure 2, together with the signal efficiencies as a function of the higgs mass. The number of expected and observed events in the $\sqrt{s} = 192 - 202$ GeV data along with the signal efficiencies, after a cut on the final variable, are shown in Table 2. The final variable is calculated for each scan point in the $(\tan\beta, m_{\mathrm{A}})$ plane. An example of the final variable distribution for the two analysis, hZ and hA, is shown in Figure 3.

The $\mathrm{hA} \to \mathrm{b\bar{b}}\tau^+\tau^-$, $\mathrm{hZ} \to \mathrm{b\bar{b}}\tau^+\tau^-$ and $\mathrm{hZ} \to \tau^+\tau^-\mathrm{q\bar{q}}$ Channels

The signatures of $\mathrm{hA} \to \mathrm{b\bar{b}}\tau^+\tau^-$[1)], $\mathrm{hZ} \to \mathrm{b\bar{b}}\tau^+\tau^-$ or $\mathrm{hZ} \to \tau^+\tau^-\mathrm{q\bar{q}}$ events are a pair of taus accompanied by two hadronic jets. The main background comes from W-pair decays containing taus. Two analyses are optimized for the hZ and for the hA channels. The hZ analysis is described in detail in Reference [19]. For $\mathrm{hA} \to \mathrm{b\bar{b}}\tau^+\tau^-$ two selections are performed, one based on the tau identification (particle-based selection) and the other relying on the event topology (jet-based selection).

First a common preselection [19] is applied, and then cuts specific to each analysis are chosen. The major difference between the hZ selection used in the Standard Model Higgs

[1)] The $\mathrm{hA} \to \tau^+\tau^-\mathrm{b\bar{b}}$ decay mode is also considered search and the hA search results from the need of high sensitivity at lower Higgs masses. To accomplish this, the cuts on opening angles of the jet and tau pairs have been removed and the cuts on invariant mass of the tau pair, $m_{\tau\tau}$, and jet pair systems, m_{qq}, have been relaxed to lie between 5 GeV and 125 GeV. To supress the additional background accepted, additional cuts are applied exploiting the kinematics of the hA events. A cut is placed on the ratio of the sum of the energies of the tau decay products over the sum of the energies of the jets, $(E^{dec}_{\tau 1} + E^{dec}_{\tau 2})/(E_{jet1} + E_{jet2})$, to be less than one. The magnitude of the missing momentum vector in the rest frame of the Higgs, p^*_{miss}, is required to be less than 40 GeV, because the taus are back-to-back leading to a partial cancellation of the missing momentum vectors. Finally, there is a requirement on the cosine of the polar angle of the Higgs boson, $|cos\theta|$, to be less than 0.8. The number of events observed, the number expected from background processes, and the signal efficiency for the two selections are shown in Table 3.

The final variable is the likelihood of the event to be either hA or hZ based on the B_{Tag} for each hadronic jet, shown in Figures 4a and 4b, and the reconstructed invariant mass of either the jet or tau pair, shown in Figures 4c and 4d, using the same technique as in the Standard Model Higgs search [14]. Events, which pass the hA as well as the hZ selection are classified as either hA or hZ depending on the values of these likelihoods. The final variable is calculated for each scan point in the ($\tan\beta$,m_A) plane. Examples of the final variable for the hA and hZ search at large values of $\tan\beta$ are shown in Figures 5.

Results

No evidence of the production of the h and A bosons is observed in the data. The region of the MSSM parameter space excluded by this data is evaluated by calculating the confidence level (CL) that the expected signal is absent in the data for the plane defined by ($\tan\beta, m_A$). The CL is calculated from the spectra of the final variables presented in the previous sections, using the technique described in References [18, 20].

Systematic and statistical errors on the signal and background are evaluated using the same procedure as in the Standard Model Higgs search [14]. The main sources of systematic error are detector resolution, selection and theoretical uncertainties. The overall systematic error is estimated to be 4% on the number of signal and 10% on the number of background events. Bins of the final variables with a signal-over-background ratio in the Monte Carlo of less than 0.05 are not considered in the calculation of CL. This cut is chosen to minimize the effect of systematic errors on the average CL as calculated from a large set of Monte Carlo experiments. Mass spectra of the most significant candidates in the hA $\rightarrow b\bar{b}b\bar{b}$ and hA $\rightarrow b\bar{b}\tau^+\tau^-$ search channels are shown in Figures 6a and 6b respectively. These spectra have been obtained after applying final selection and tight cut on B_{tag} for the tau channels, and applying a cut on the final variable NN > 0.9 for the four jets channels.

The data from the MSSM Higgs search using lower center-of-mass energies [2] is combined with the results presented in this paper. Figure 7 shows the region of the ($\tan\beta$,m_h) plane and ($\tan\beta$,m_A) plane excluded by L3 for the maximal mixing and no mixing scenarios. In the plots, the 95% CL is shown as a solid line while the expected median CL is shown as a dashed line.

For the MSSM parameters considered and assuming $\tan\beta$ greater than 0.8, this results in a lower mass limits at the 95% CL of

$$m_h > 82.6 \text{ GeV}, \quad m_A > 83.0 \text{ GeV}.$$

The median expected limits in the absence of a signal are $m_{\mathrm{h}} > 85.3$ GeV and $m_{\mathrm{A}} > 86.4$ GeV.

As can be seen from the exclusion plots for the no mixing scenario there is a small unexcluded area in the low tanβ region at low values of m_{A} where the decay $\mathrm{h} \rightarrow \mathrm{AA}$ opens. This decay mode is not considered in our analysis of the data collected at 192 - 202 GeV. That's why the search sensitivity deteriorates in the region of the MSSM parameter space where branching ratio of the mentioned decay mode becomes sizable.

For $0.8 < \tan\beta < 1.6$ values of m_{A} up to 1 TeV are ruled out regardless of mixing scheme thus leading to exclusion of this tanβ region in the MSSM.

Acknowledgments

We acknowledge the efforts of the engineers and technicians who have participated in the construction and maintenance of L3 and express our gratitude to the CERN accelerator divisions for the superb performance of LEP.

References

[1] H. P. Nilles, Phys. Rep. **110** (1984) 1.

H. E. Haber and G. L. Kane, Phys. Rep. **117** (1985) 75.

R. Barbieri, Riv. Nuovo Cim. **11 n°4** (1988) 1.

[2] L3 Collaboration, M. Acciarri and others, Phys. Lett. **B 471** (1999) 321.

[3] OPAL Collaboration, G. Abbiendi and others, Eur. Phys. Jo. **C 7** (1999) 407.

ALEPH Collaboration, R. Barate and others, Phys. Lett. **B 440** (1998) 419.

DELPHI Collaboration, P. Abreu and others, "Search for neutral Higgs bosons in e^+e^- collisions at $\sqrt{s} = 183$ GeV", Preprint EP/99-006, CERN, 1999, Accepted for publication by E. Phys. J. **C**.

[4] L3 Collaboration, B. Adeva and others, Nucl. Inst. Meth. **A 289** (1990) 35.

J. A. Bakken and others, Nucl. Inst. Meth. **A 275** (1989) 81.

O. Adriani and others, Nucl. Inst. Meth. **A 302** (1991) 53.

B. Adeva and others, Nucl. Inst. Meth. **A 323** (1992) 109.

K. Deiters and others, Nucl. Inst. Meth. **A 323** (1992) 162.

M. Chemarin and others, Nucl. Inst. Meth. **A 349** (1994) 345.

M. Acciarri and others, Nucl. Inst. Meth. **A 351** (1994) 300.

G. Basti and others, Nucl. Inst. Meth. **A 374** (1996) 293.

A. Adam and others, Nucl. Inst. Meth. **A 383** (1996) 342.

[5] P. Janot, *The HZHA Generator* in G. Altarelli, T. Sjöstrand, F. Zwirner,*Physics at LEP2*, CERN 96-01, 1996, vol. 2, p.309, version 3, released in December 1999, http://alephwww.cern.ch/janot/Generators.html.

[6] T. Sjöstrand, "PYTHIA", Preprint TH/93-7112, CERN, 1993, Revised August 1995.

T. Sjöstrand, Comp. Phys. Comm. **82** (1994) 74.

[7] M. Skrzypek and others, Comp. Phys. Comm. **94** (1996) 216.

M. Skrzypek and others, Phys. Lett. **B 372** (1996) 289.

[8] S. Jadach and B. F. L. Ward and Z. Wąs, Comp. Phys. Comm. **66** (1991) 276.

[9] R. Engel, Z. Phys. **C 66** (1995) 203.

R. Engel and J. Ranft and S. Roesler, Phys. Rev. **D 52** (1995) 1459.

[10] F. A. Berends and R. Pittau and R. Kleiss, Comp. Phys. Comm. **85** (1995) 437.

[11] R. Brun and others, "GEANT 3", CERN DD/EE/84-1, Revised 1987.

[12] H. Fesefeldt, "GHEISHA", Preprint PITHA 85/02, RWTH Aachen, 1985.

[13] M. Carena, S. Heinemeyer, C.E.M. Wagner and G. Weiglein, *Suggestions for Improved Benchmark Scenarios for Higgs Boson Searches at LEP2*, CERN-TH/99-374, DESY 99-186,hep-ph/9912223.

[14] L3 Collaboration, M. Acciarri and others, "Search for the Standard Model Higgs boson in e^+e^- interactions at $\sqrt{s} = 192-202$ GeV", Preprint EP/00-XXX, CERN, 2000, Submitted for publication by Phys. Lett. B.

[15] L3 Collaboration, M. Acciarri and others, Phys. Lett. **B 436** (1998) 389.

[16] S. Bethke and others, Nucl. Phys. **B 370** (1992) 310.

[17] L. Lönnblad and C. Peterson and T. Rognvaldsson, Nucl. Phys. **B 349** (1991) 675.
C. Peterson and others, Comp. Phys. Comm. **81** (1994) 185.

[18] L3 Collaboration, M. Acciarri and others, Phys. Lett. **B 411** (1997) 373.

[19] L3 Collaboration, M. Acciarri and others, "Search for the Standard Model Higgs boson in e^+e^- interactions at $\sqrt{s} = 189$ GeV", Preprint EP/99-080, CERN, 1999, Accepted for publication by Phys. Lett. B.

[20] A. Favara and M. Pieri, "Confidence Level Estimation and Analysis Optimization", Preprint, INFN University of Florence, 1997, DFF-278-4-1997.

[21] G. Alexander *et al.*, Z. Phys. **C73** (1997) 189.

192 GeV	Preselection	NN(hA) >0.9	NN(hZ) >0.5
$e^+e^- \to q\bar{q}$	201.2	0.4	3.0
$e^+e^- \to W^+W^-$	217.9	0.2	4.2
$e^+e^- \to ZZ$	14.5	0.4	2.3
Total	433.6	1.0	9.5
Data	430	2	4
Efficiency $hA \to b\bar{b}b\bar{b}$	95.0%	42.0%	-
Efficiency $hZ \to b\bar{b}q\bar{q}$	93.7%	-	52.7%
196 GeV	Preselection	NN(hA) >0.9	NN(hZ) >0.5
$e^+e^- \to q\bar{q}$	531.3	1.2	7.1
$e^+e^- \to W^+W^-$	622.3	0.7	11.9
$e^+e^- \to ZZ$	43.9	1.3	7.0
Total	1197.5	3.2	26.0
Data	1186	3	33
Efficiency $hA \to bbbb$	95.0%	42.0%	-
Efficiency $hZ \to b\bar{b}q\bar{q}$	93.7%	-	52.7%
200 GeV	Preselection	NN(hA) >0.9	NN(hZ) >0.5
$e^+e^- \to q\bar{q}$	478.3	0.7	2.5
$e^+e^- \to W^+W^-$	595.4	0.3	3.3
$e^+e^- \to ZZ$	44.7	1.0	3.3
Total	1118.4	2.0	9.1
Data	1198	2	9
Efficiency $hA \to bbbb$	94.1%	37.9%	-
Efficiency $hZ \to b\bar{b}q\bar{q}$	91.0%	-	40.9%
202 GeV	Preselection	NN(hA) >0.9	NN(hZ) >0.5
$e^+e^- \to q\bar{q}$	215.0	0.3	1.5
$e^+e^- \to W^+W^-$	271.8	0.2	1.7
$e^+e^- \to ZZ$	21.0	0.5	1.6
Total	507.8	1.0	4.8
Data	506	1	6
Efficiency $hA \to b\bar{b}b\bar{b}$	95.9%	38.3%	-
Efficiency $hZ \to b\bar{b}q\bar{q}$	92.3%	-	36.3%

Table 2: Number of events expected and observed in the four-jets channels, after preselection and after cuts on the final variables which give a similar discriminating power. The signal efficiencies are quoted for hA at $m_A = m_h = 85$ GeV. For hZ the efficiencies are quoted for $m_h = 100$ GeV at $\sqrt{s} = 192 - 196$ GeV and $m_h = 105$ GeV at $\sqrt{s} = 200 - 202$ GeV.

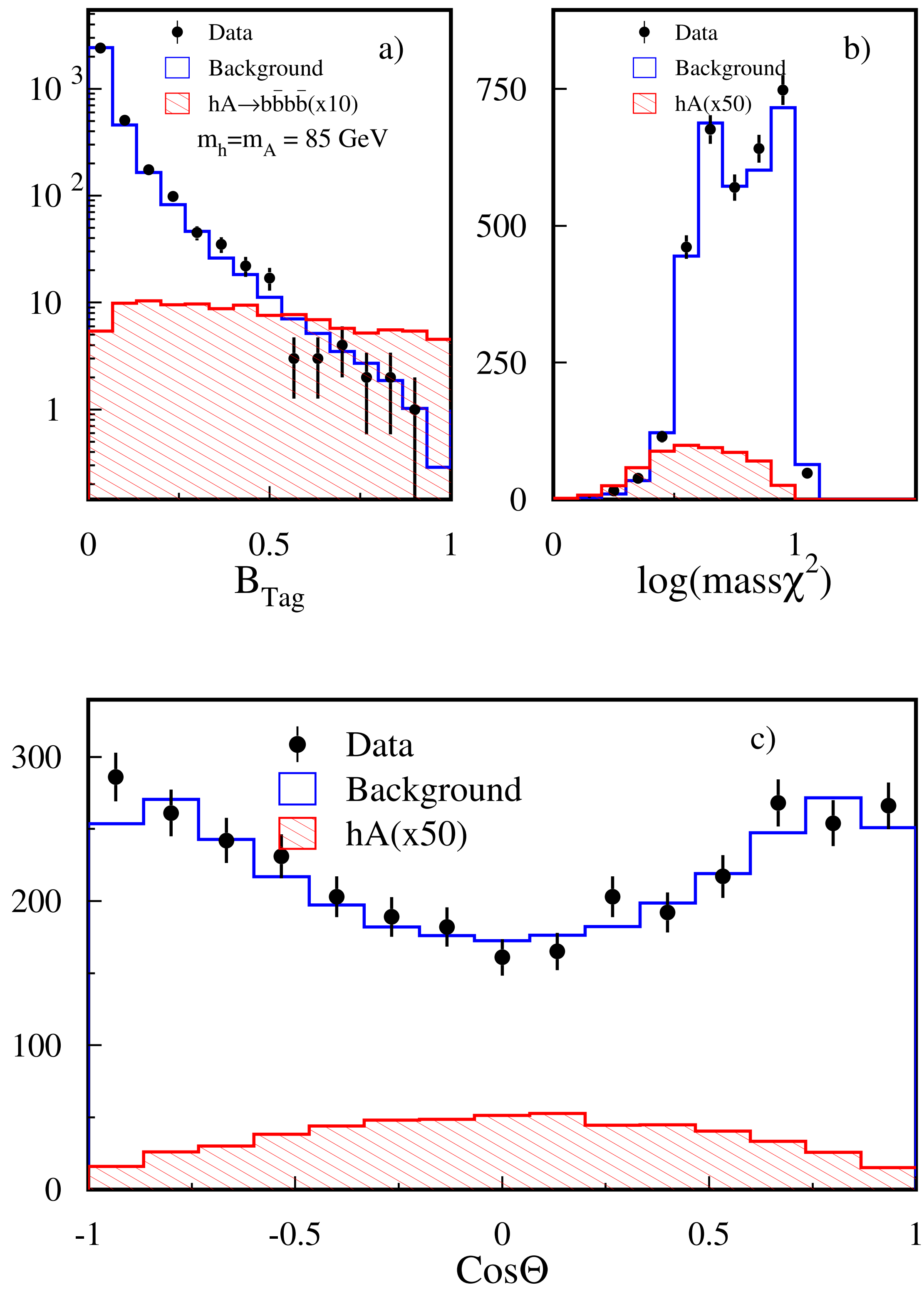

Figure 1: Distributions of the a) B_{Tag}, b) mass χ^2 and c) cosine of the polar angle of Higgs boson $\cos\theta$ in four-jet search after preselection. The dots are the observed data at $\sqrt{s} = 192{-}202$ GeV, the open histograms are the expected SM background, and the hatched histograms are the expected hA $\rightarrow$ b$\bar{\text{b}}$q$\bar{\text{q}}$ signal for $m_{\text{h}} = 85$ GeV at tan$\beta = 50$. For the B_{Tag} the expected signal is multiplied by factor 10, for the distribution of the cosine of the production angle and of the $\log(\chi^2)$, the expected signal is multiplied by a factor of 50.

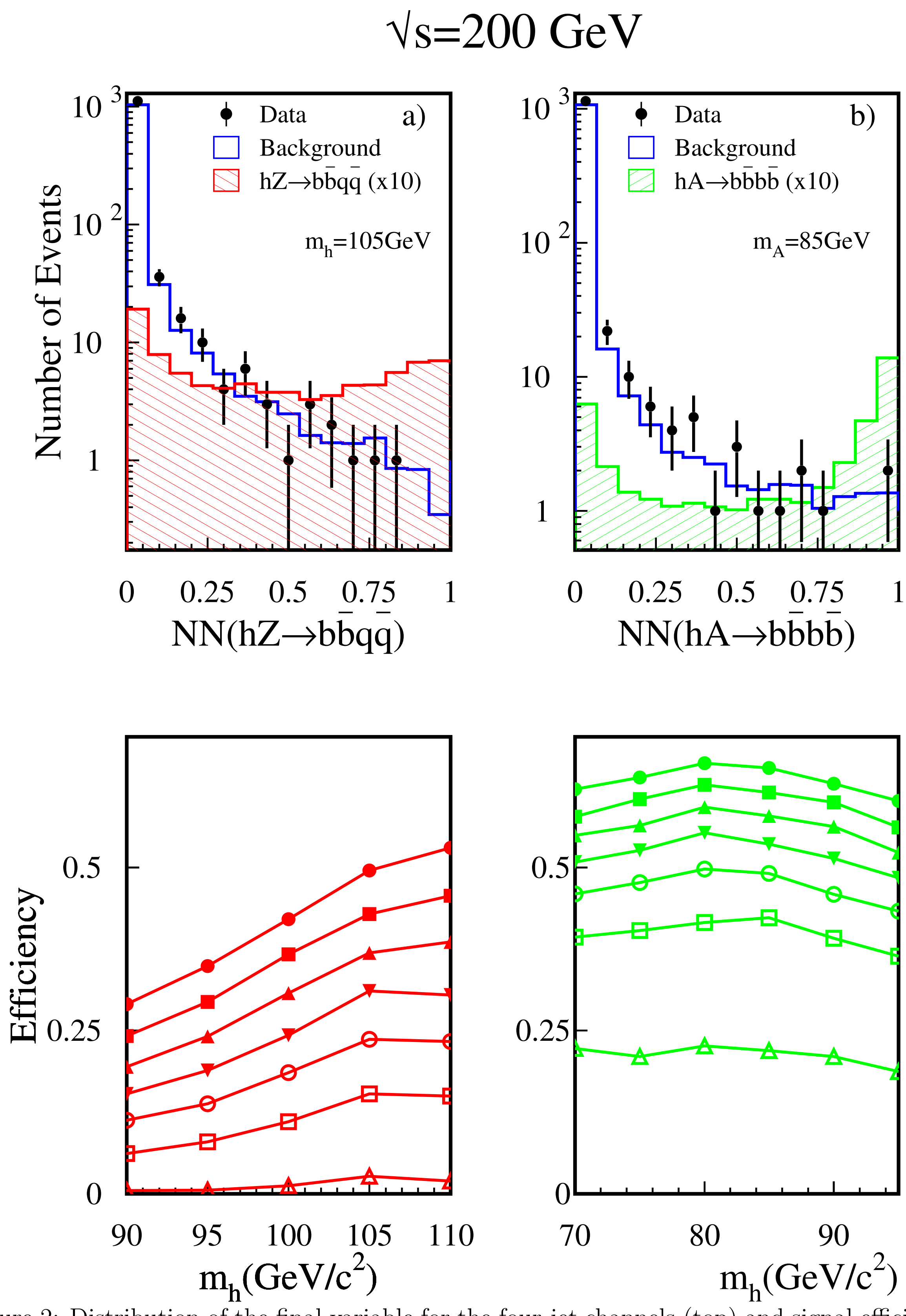

Figure 2: Distribution of the final variable for the four-jet channels (top) and signal efficiencies as a function of the higgs mass (bottom), for different cuts on the final variable from $\mathbf{NN} > \mathbf{0.37}$ (black dots) to $\mathbf{NN} > \mathbf{0.97}$ (open triangles) with 0.1 steps. The final variables are constructed assuming m_{h} =105GeV m_{A} =85 GeV.

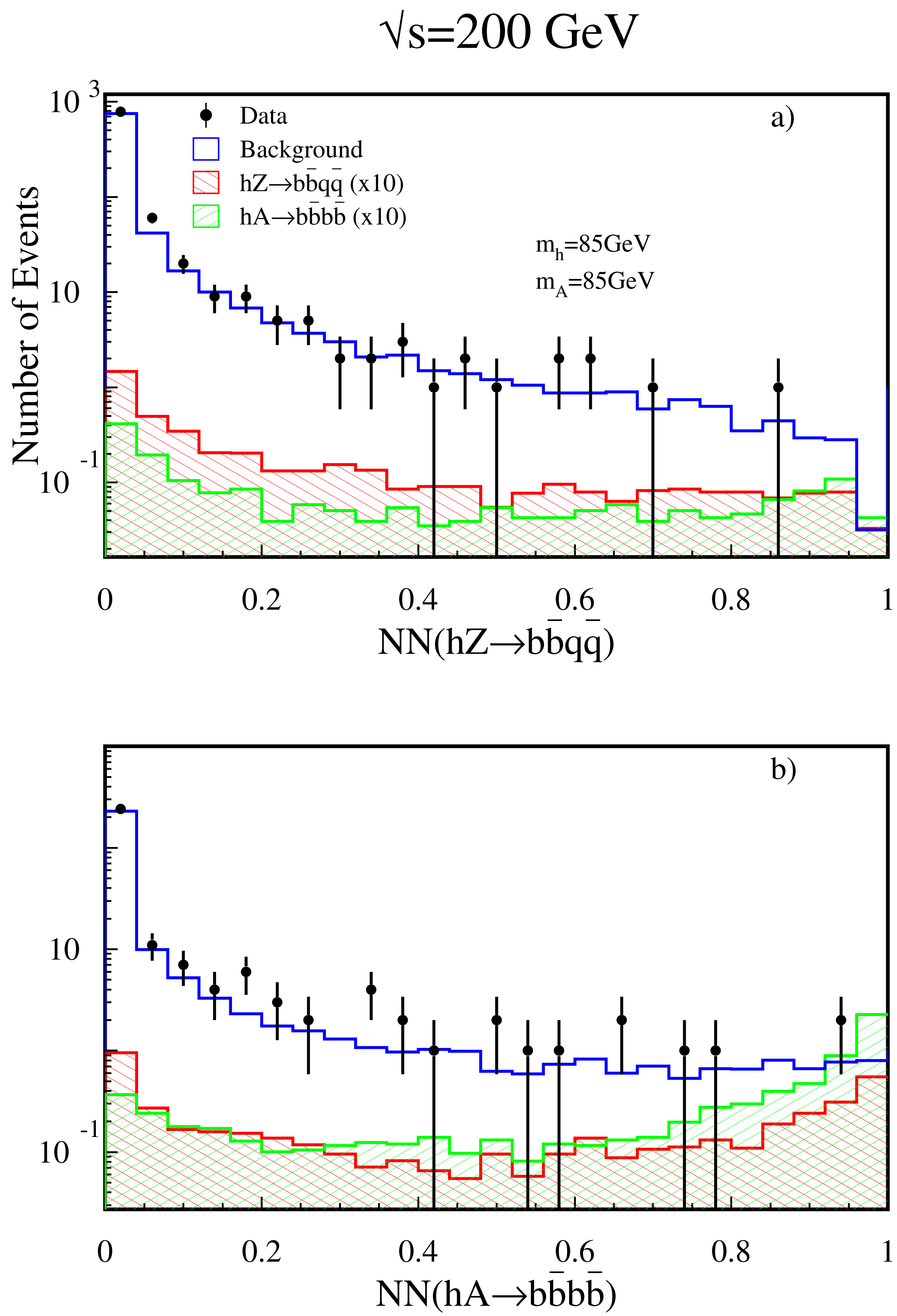

Figure 3: Distributions of the final variable for the two categories $hZ_{b\bar{b}q\bar{q}}$ (top) and $hA_{b\bar{b}b\bar{b}}$ (bottom). The final variables are constructed assuming equal mass hypothesis $m_h = m_A = 85$ GeV at high tanβ values.

192 GeV	hA cuts	hZ cuts
$e^+e^- \to q\bar{q}$	0.3	0.5
$e^+e^- \to W^+W^-$	1.8	1.8
$e^+e^- \to ZZ$	0.5	0.6
$e^+e^- \to Ze^+e^-$	0.	0.1
Total	2.6	3.0
Data	2	2
Efficiency $hA \to bb\tau^+\tau^-$	36%	36%
Efficiency $hZ \to b\bar{b}\tau^+\tau^-$	21%	29%
Efficiency $hZ \to \tau^+\tau^- q\bar{q}$	20%	31%
196 GeV	hA cuts	hZ cuts
$e^+e^- \to q\bar{q}$	0.8	1.4
$e^+e^- \to W^+W^-$	5.0	5.0
$e^+e^- \to ZZ$	1.4	1.7
$e^+e^- \to Ze^+e^-$	0.1	0.2
Total	7.3	8.4
Data	6	7
Efficiency $hA \to b\bar{b}\tau^+\tau^-$	36%	36%
Efficiency $hZ \to b\bar{b}\tau^+\tau^-$	21%	29%
Efficiency $hZ \to \tau^+\tau^- q\bar{q}$	20%	31%
200 GeV	hA cuts	hZ cuts
$e^+e^- \to q\bar{q}$	0.9	0.8
$e^+e^- \to W^+W^-$	4.6	4.7
$e^+e^- \to ZZ$	1.6	1.8
$e^+e^- \to Ze^+e^-$	0.1	0.3
Total	7.2	7.6
Data	5	7
Efficiency $hA \to bb\tau^+\tau^-$	33%	34%
Efficiency $hZ \to b\bar{b}\tau^+\tau^-$	17%	29%
Efficiency $hZ \to \tau^+\tau^- q\bar{q}$	20%	29%
202 GeV	hA cuts	hZ cuts
$e^+e^- \to q\bar{q}$	0.4	0.3
$e^+e^- \to W^+W^-$	2.0	2.1
$e^+e^- \to ZZ$	0.7	0.8
$e^+e^- \to Ze^+e^-$	0.	0.1
Total	3.2	3.4
Data	3	3
Efficiency $hA \to b\bar{b}\tau^+\tau^-$	33%	34%
Efficiency $hZ \to b\bar{b}\tau^+\tau^-$	17%	29%
Efficiency $hZ \to \tau^+\tau^- q\bar{q}$	20%	29%

Table 3: Number of events expected and observed after selection for the tau search channels. The signal efficiencies are quoted for hA at $m_A = m_h = 85$ GeV. For hZ the efficiencies are quoted for $m_h = 100$ GeV at $\sqrt{s} = 192..196$ GeV and for $m_h = 105$ GeV at $\sqrt{s} = 200..202$ GeV.

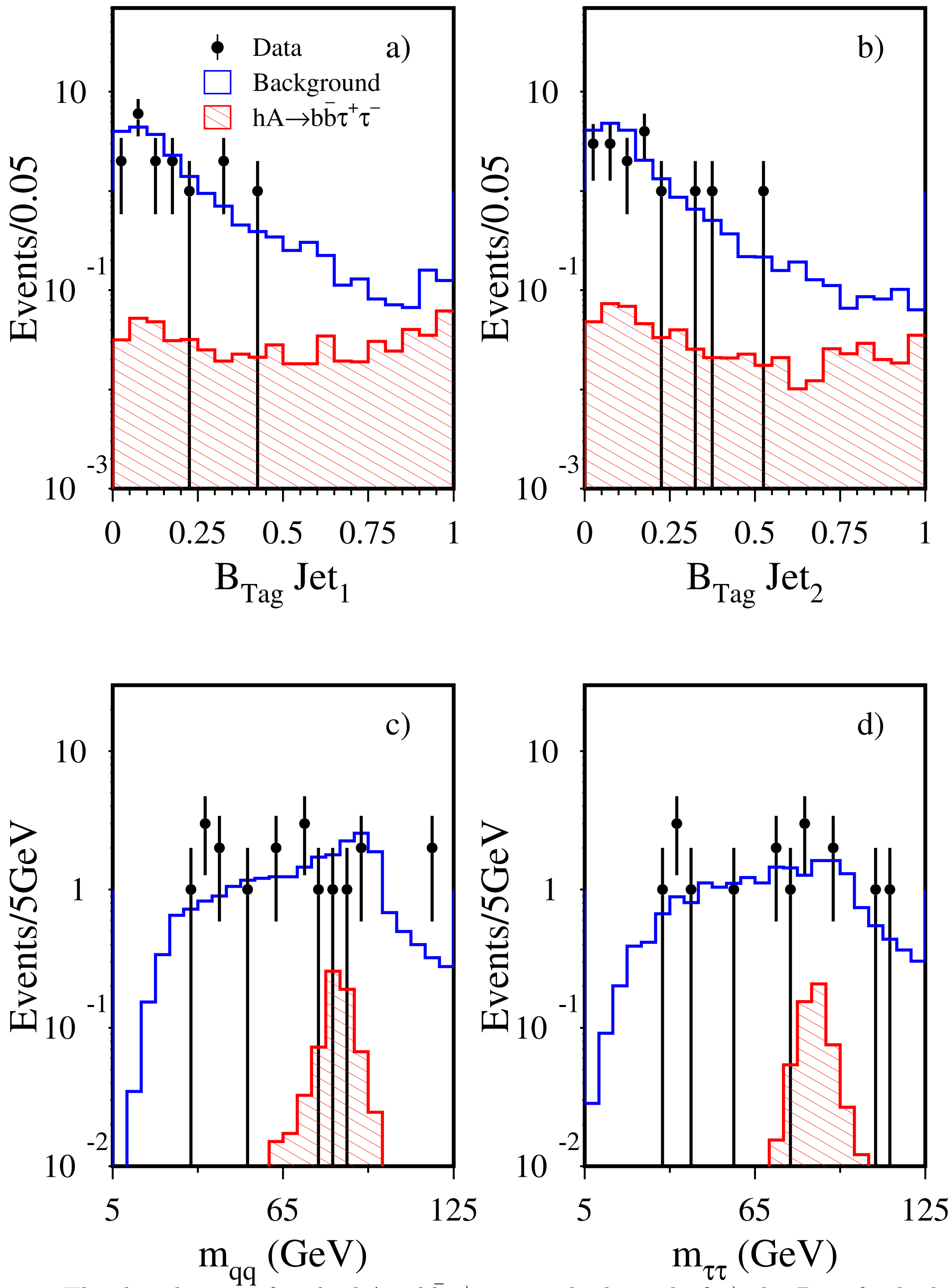

Figure 4: The distributions for the $\mathrm{hA}\rightarrow\mathrm{b\bar{b}}\tau^+\tau^-$ search channel of a) the $\mathrm{B_{Tag}}$ for hadronic jet 1 and b) hadronic jet 2, c) the reconstructed mass for the hadronic system, and d) the reconstructed mass for the leptonic system. The dots are the $\sqrt{s} = 192 - 202$ GeV data, the open histograms the Monte Carlo background and the hatched histograms the expected $\mathrm{hA}\rightarrow\mathrm{b\bar{b}}\tau^+\tau^-$ signal for $m_\mathrm{h} = 85$ GeV and $\tan\beta = 50$.

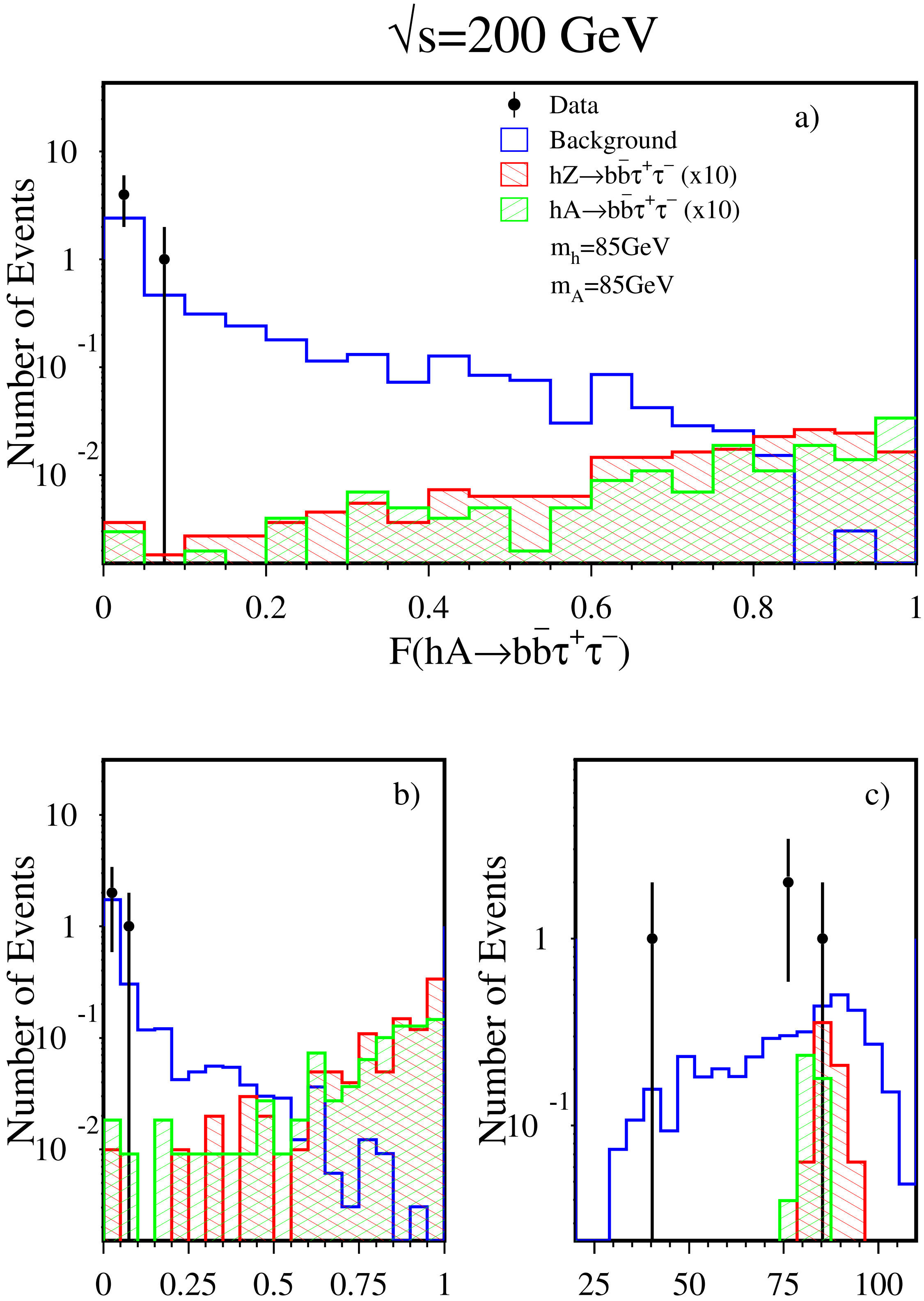

Figure 5: Distributions of the final variables for the a) $\mathrm{hA}\to \mathrm{b\bar{b}}\tau^+\tau^-$ b) the $\mathrm{hZ}\to \mathrm{b\bar{b}}\tau^+\tau^-$ and c) the $\mathrm{hZ}\to\tau^+\tau^-\mathrm{q\bar{q}}$ search for $m_\mathrm{h} = m_A = 85$ GeV at high $\tan\beta$. Dots are data collected at 200 GeV, open histogramms are expected SM background, hatched histogramms are signal efficiencies for hZ and hA search multiplied by factor 10.

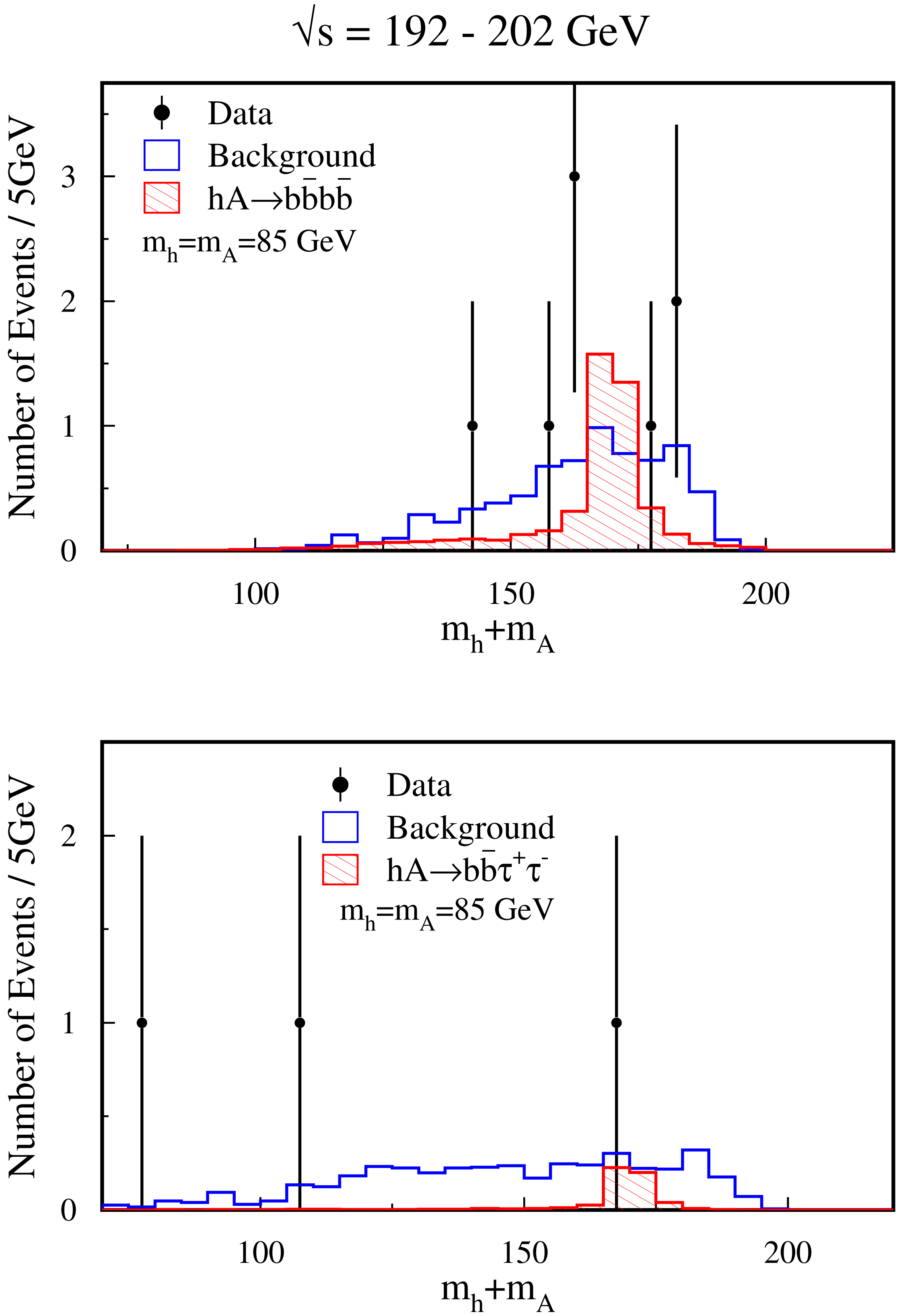

Figure 6: Most significant candidates. Top: Reconstructed dijet mass sum in the $\mathrm{hA} \rightarrow \mathrm{b\bar{b}b\bar{b}}$. Bottom: Sum of the dijet and the ditau mass in the $\mathrm{hA} \rightarrow \mathrm{b\bar{b}}\tau^{+}\tau^{-}$ channel.

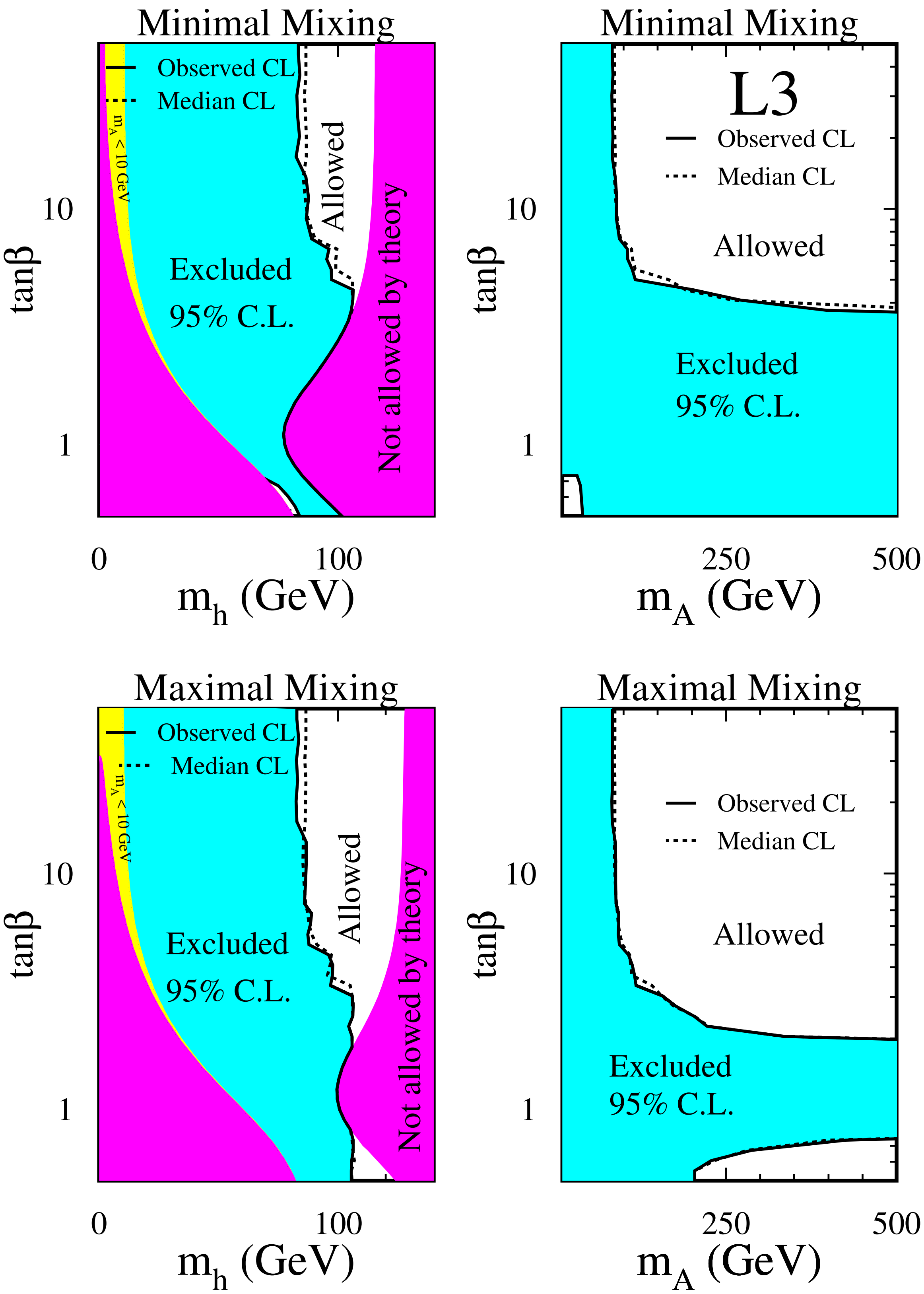

Figure 7: Exclusion plots in ($\tan\beta$,m_h) and ($\tan\beta$,m_A) planes at the 95% CL for maximal mixing and minimal mixing scenarios. The grey area is the 95% exclusion, the black area in ($\tan\beta$,m_h) plane is a theoretically disallowed region. The light grey area corresponds to $m_\mathrm{A} < 10$ GeV and has been previously excluded at LEP [21].